Short communication

Allyl ethyl carbonate as an additive for lithium-ion battery electrolytes

Jyh-Tsung Lee*, Yueh-Wei Lin, Yih-Song Jan

[a] *Materials Research Laboratories, Industrial Technology Research Institute, Chutung, Hsinchu, 31040 Taiwan, ROC*

Abstract

The role of allyl ethyl carbonate (AEC) as an additive in electrolytes used in lithium-ion batteries is investigated. The 1.0 M $LiPF_6$ in propylene carbonate (PC): diethyl carbonate (DEC) (3:2 in volume) electrolyte containing AEC can suppress the co-intercalation of PC and inhibit the decomposition of electrolytes during the first lithium intercalation. A graphitic anode (MCMB-2528, mesocarbon microbeads) in a PC-based electrolyte exhibits a high reversible capacity of 320 mAh g^{-1}. The reduction potential of AEC is 1.5 V versus Li|Li$^+$ as determined by cyclic voltammetry (CV). The morphology and structure of graphite electrodes after the first charge–discharge cycle are investigated by scanning electron microscopy (SEM) and X-ray powder diffraction (XRD). AEC decomposes and forms a proper solid electrolyte interphase (SEI) film on the MCMB surface. The SEI film not only prevents exfoliation of the graphite electrode but also stabilizes the electrolyte. AEC helps to improve the cycleability of lithium-ion batteries to a considerable extent.
© 2004 Elsevier B.V. All rights reserved.

Keywords: Allyl ethyl carbonate; Additive; Solid electrolyte interphase; Lithium-ion battery; Reversible capacity; Cycleability

1. Introduction

Highly graphitized carbonaceous materials have been used as anode electrodes in commercial lithium-ion batteries [1,2]. The electrolytes typically consist of a lithium salt dissolved in organic solvents. Organic carbonates are the preferred class of solvent class in commercial batteries, e.g. ethylene carbonate (EC) and EC– propylene carbonate (PC) mixed solvents. Nevertheless, EC has a poor low-temperature performance due to its high melting point (about 37 °C). By contrast, PC has many advantages over the carbonates because of its higher dielectric constant and better low-temperature performance (PC has a lower melting point of −49 °C). Unfortunately, PC co-intercalates with lithium ions into graphene layers, and hence subsequent exfoliation of the graphite is observed [3,4].

Recently, several researchers have investigated additives that will suppress the decomposition of PC to promote the performance of lithium-ion batteries. The additives will helpfully generate an effective solid electrolyte interphase (SEI) film to prevent the co-intercalation of PC and the decomposition of electrolytes. The SEI films also play a beneficial role in improving the safety and cycleability of lithium-ion batteries. Several additives have been reported, e.g. CO_2 [5–8], N_2O [5], SO_2 [9,10], S_x^{2-} [5,11], vinylene carbonate (VC) [12], ethylene sulfite (ES) [13], propylene sulfite (PS) [14], 1,3-benzodioxol-2-one [15], and halogenated additives [16,17].

In this paper, allyl ethyl carbonate (AEC) is examined as a new additive for electrolytes in lithium-ion batteries. The performance of the batteries is improved by PC-based electrolytes with AEC additive.

2. Experimental

The graphite anode consisted of 93% mesocarbon microbeads (MCMB)-2528 (graphitized mesocarbon microbeads at 2800°C, Osaka Gas) and 7% polyvinylidene difluoride (PVdF) as a binder. The electrolyte was 1.0 M $LiPF_6$ in a PC:DEC (3:2 in volume) mixed solvent with or without 2 wt.% AEC as an additive. The water content of the electrolytes determined by Karl Fisher titration was about 20 ppm.

In a coin cell, lithium metal foil was use for the counter and reference electrodes, and the graphite electrode served as the anode. The cells were cycled at a constant current at the 0.2 C rate between 0.01 and 1.8 V.

The morphology of the graphite electrodes was observed by scanning electron microscopy (SEM) on a CamScan microscopy using an accelerating voltage of 20 kV. The samples were uncoated. X-ray powder diffraction (XRD) studies

* Corresponding author. Tel.: +886-3-591-8206; fax: +886-3-582-0442.
E-mail address: jtlee@itri.org.tw (J.-T. Lee).

of films of the MCMB electrode were obtained by means of a Shimadzu XD-5 X-ray diffractometer with a Cu K$_\alpha$ ($\lambda = 1.54178$ Å).

3. Results and discussion

3.1. Charge and discharge of Li/graphite cell

For the Li|graphite cell, the first charge–discharge voltage curves of a graphite electrode in a 1.0 M LiPF$_6$–PC:DEC (3:2 in volume) electrolyte with or without 2 wt.% AEC as an additive are shown in Fig. 1. For the cell containing a 1.0 M LiPF$_6$–PC/DEC electrolyte, the first discharge curve (Fig. 1(a)) is a long plateau at about 0.77–0.84 V (versus Li|Li$^+$), which indicates that decomposition of PC is taking place [3]. For the cell containing 2 wt.% AEC, however the discharge curve decreases dramatically to near 0 V (Fig. 1(b)), which indicates that electrochemical decomposition of PC is suppressed by AEC. This is probably due to the decomposition products of the fact that the additive form a SEI film on the MCMB surface. The cycle-life of the above cell is shown in Fig. 2. The graphite electrode displays good rechargeability with a reversible capacity of 320 mAh g^{-1}. Interestingly, the irreversible capacity of the first cycle is high (about 80 mAh g^{-1}) due to SEI film formation on the MCMB surface. This observation is in agreement with the findings of other works [15].

3.2. Reduction potential of electrolyte solvents

To obtain information on SEI film formation, the reduction potential of the electrolyte solvent was observed by cyclic voltammetry (CV) with a slow scan. Voltammograms between 2 and 0.01 V at 0.02 mV s^{-1} in a 0.1 M
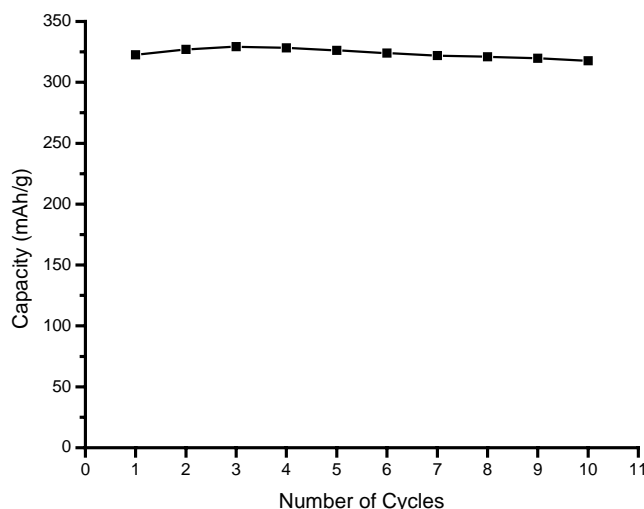
Fig. 2. Discharge capacity as a function of cycle number for MCMB-2528 electrode in a 1.0 M LiPF$_6$–PC:DEC (3:2, v/v) electrolyte with 2 wt.% AEC as an additive at 0.2 C rate charge–discharge cycling.

LiPF$_6$–PC:DEC (=3:2) electrolyte with 0, 2, 5 and 10 wt.% of AEC additive, respectively, are shown in Fig. 3. In the PC-based electrolyte, a large reduction peak at 0.7–0.8 V is present in the first cycle (Fig. 3(a)). This confirms decomposition of the electrolytes. In the presence of 2 wt.% AEC, the reduction peak at 0.7 V is reduced and a small peak appears at 1.5 V due to the reduction of AEC. Moreover, as the content of AEC is increased to 5 or 10 wt.%, the reduction peak at 0.7 V, corresponding to the decomposition of electrolyte, is decreased. This further proves that decomposition of the electrolyte is suppressed when AEC is used as an additive. In the reduction decomposition mechanism of carbonates, it is believed that one-electron transfer to oxygen results in breakage of the C–O bond [18], as shown in Scheme 1, to form an anion and a radical. Allylic radicals are stabilized by resonance hybridization. Overlap with the p orbitals of a π bond allows the odd electron to delocalize over two carbon atoms (Scheme 2). Resonance delocalization is particularly effective in stabilizing radicals, in the order of benzylic ∼ allylic > tertiary (3°) > secondary (2°) > primary (1°) [19]. Since AEC has the driving force to form a more stable allylic radical, its decomposition is highly favoured. AEC forms a SEI film at a higher reduction potential (about 1.5 V) than other electrolytes such as PC and DEC. This prevents the co-intercalation of PC and the decomposition of electrolytes.

3.3. First charge–discharge of graphite electrode

It has been widely recognized that a SEI film is formed during the first charge–discharge cycle. In order to observe SEI film formation, graphite electrodes have been cycled in electrolyte with and without AEC and then visually inspected. In the absence of AEC, the electrode appeared to be virtually unchanged. By contrast, in the presence of AEC,
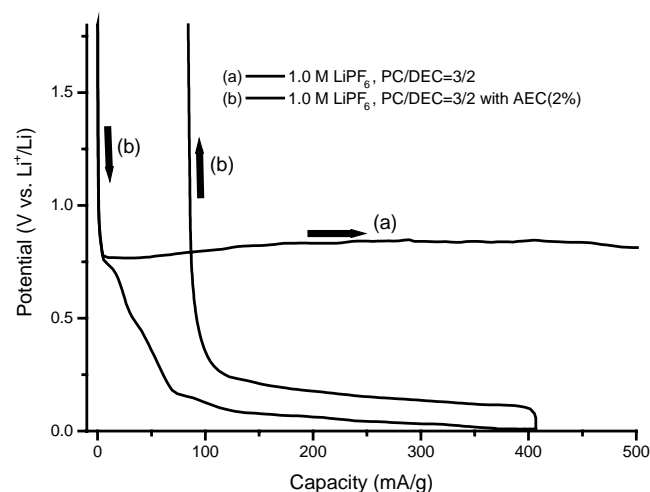

Fig. 1. First cycle constant-current, charge–discharge characteristics of MCMB-2528 in a 1.0 M LiPF$_6$–PC:DEC (3:2, v/v) electrolyte: (a) without any additive and (b) with 2 wt.% AEC as an additive.
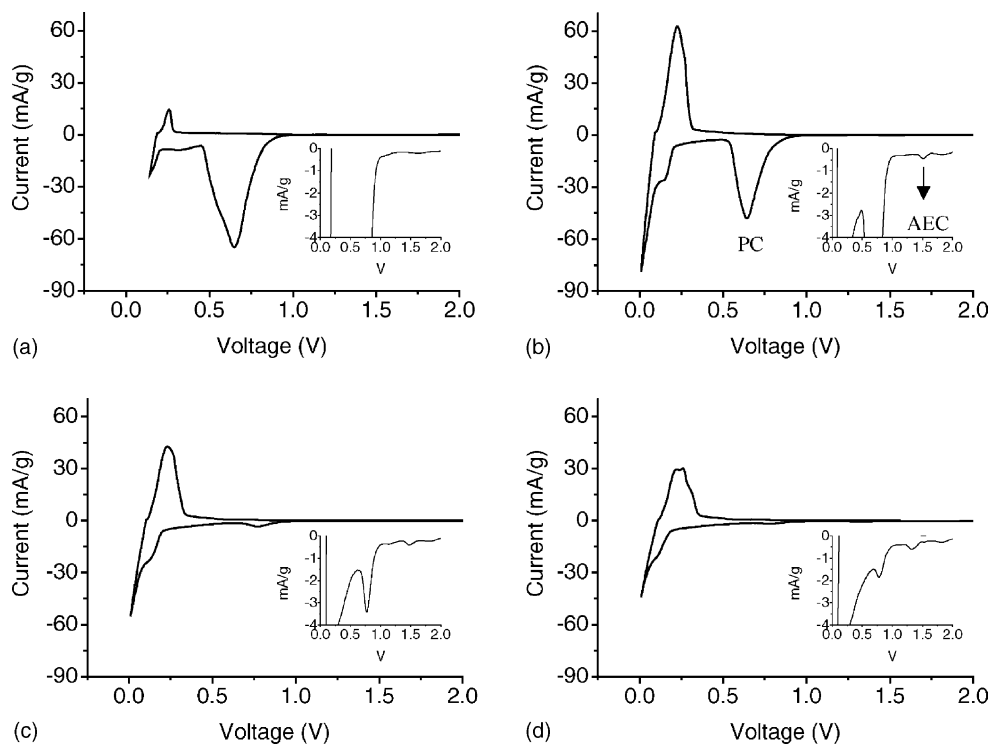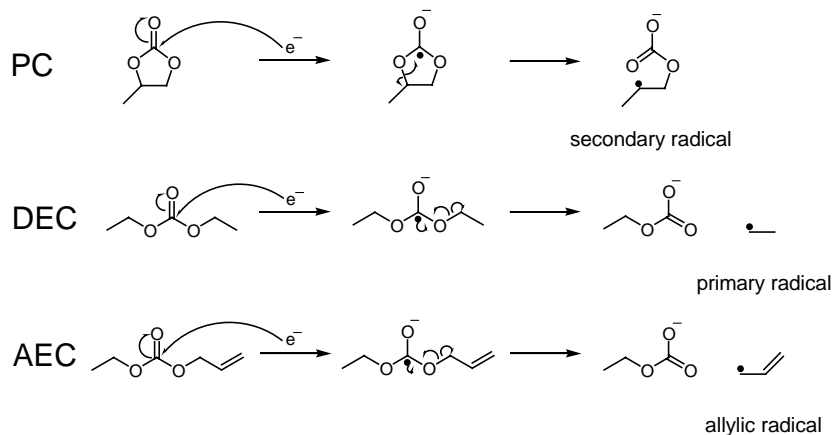
Fig. 3. Cyclic voltammograms of MCMB-2528 electrode in 0.1 M LiPF$_6$–PC:DEC (3:2, v/v) electrolyte with (a) 0 wt.% (blank), (b) 2 wt.%, (c) 5 wt.% and (d) 10 wt.% AEC as additive at sweep rate of 0.02 mV s^{-1}.

Scheme 1.

it was found that the graphite had electrode exfoliated after the first discharge process. To gain a better understanding of the SEI film on MCMB, the graphite electrodes were inspected after the first charge–discharge cycle, and were then analyzed with SEM. Interestingly, the SEM results show that
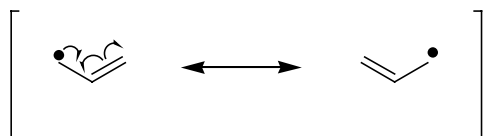
Scheme 2.

the growth of the film on the MCMB surface is significant (Fig. 4(b)). The original smooth surface of graphite electrode (Fig. 4(a), inset) turns rough and is covered with films that have a nodular morphology (Fig. 4(b), inset). To explore further the possible formation of SEI films, a control experiment was conducted with the same electrodes and the electrolyte without AEC additive. The original ball shape of the MCMB disappears, and the morphology of MCMB becomes plate-like (Fig. 4(c)). Such changes in shape may be due to co-intercalation of PC with lithium ions, which often leads to a drastic increase in volume (>100%) [20]. The decomposition of electrolyte at about 0.8 V during the charge process has been found to generate gaseous products
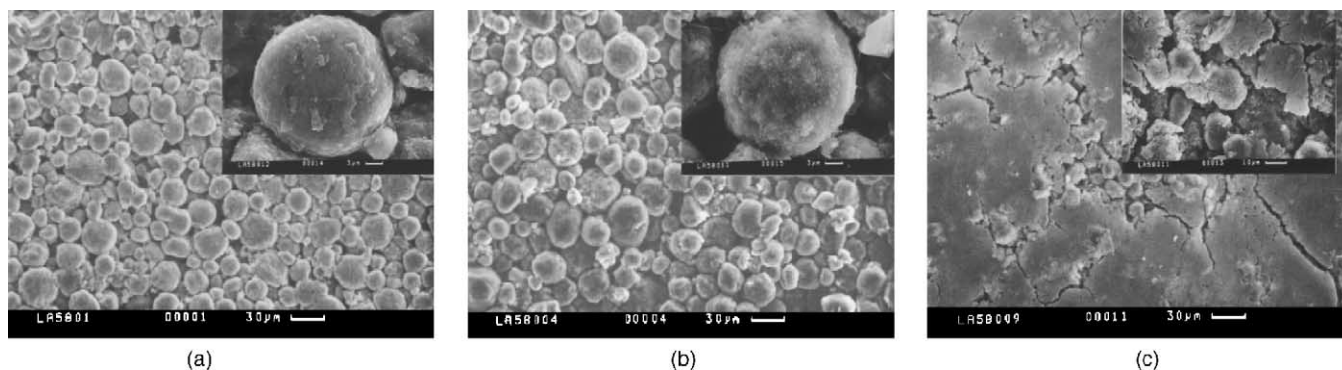
Fig. 4. SEM micrographs for (a) original MCMB-2528 electrode, (b) MCMB-2528 electrode in 1.0 M LiPF$_6$–PC:DEC (3:2, v/v) electrolyte with 2 wt.% AEC additive, and (c) without any additive after first cycle.

such as propylene gas, carbon monoxide and carbon dioxide [21]. The structure of the graphite is destroyed during the first charging process when PC-based electrolytes are used without any additive. It is believed that AEC in the first intercalation may have decomposed and formed a good quality SEI film on graphite negative electrode via the reductive decomposition of electrolyte solutions. The electrolyte with 2 wt.% AEC can suppress the co-intercalation of PC which, in turn, inhibits the decomposition of electrolytes.

The structure of the above electrodes was also investigated with XRD. The XRD pattern (Fig. 5(a)) for an original electrode shows four intense diffraction peaks at $2\theta =$ 26.36, 50.44, 54.64 and 74.12°. The corresponding d spacing of these peaks is calculated to be 3.381, 1.809, 1.680 and 1.279 Å, which is consistent with the respective d spacing for C(0 0 2), Cu(2 0 0), C(0 0 4) and Cu(2 2 0) peaks [22]. The XRD results show that the diffraction peaks consist of MCMB-2528 and Cu foil (fcc) as a substrate. Interestingly, the XRD pattern (Fig. 5(b)) for the electrode in a 1.0 M LiPF$_6$–PC based electrolyte with AEC additive has a I_{002}/I_{220} of 1.28, which is similar to 1.29 for the original

electrode. The area ratio of the C(0 0 2) peak relative to the Cu(2 2 0) peak decreases from 1.29 (original electrode) to 0.85 (electrolyte without any additive is shown in Fig. 5(c)). This confirms the structural transformation from a highly ordered graphitic phase to a more disordered, amorphous, carbon phase.

The XRD studies supplement the observations of SEM. They show that the graphite electrode exfoliates in PC-based electrolytes without any additive due to the co-intercalation of PC. Apparently, AEC as an additive can form a SEI film to prevent the graphite exfoliation and electrolyte decomposition.

4. Conclusions

AEC has higher reduction potential, viz., 1.5 V, than either PC or DEC electrolytes and therefore easily forms a SEI film of good quality. This is due to the formation of a stable allylic radical after the decomposition of AEC. The resultant SEI film can suppress the co-intercalation of PC and the decomposition of electrolytes. The PC-based electrolytes with 2 wt.% AEC as an additive enhance the performance of lithium-ion batteries.

Fig. 5. XRD patterns of (a) original MCMB-2528 electrode, (b) MCMB-2528 electrode in 1.0 M LiPF$_6$–PC:DEC (3:2, v/v) electrolyte with 2 wt.% AEC additive, and (c) without any additive after first cycle.

References

[1] Z. Ogumi, M. Inaba, Bull. Chem. Soc. Jpn. 71 (1998) 521.
[2] M. Winter, J.O. Besenhard, M.E. Spahr, P. Novak, Adv. Mater. 10 (1998) 725.
[3] A.N. Dey, B.P. Sullivan, J. Electrochem. Soc. 117 (1970) 222.
[4] J.O. Besenhard, H.P. Fritz, J. Electroanal. Chem. 53 (1974) 329.
[5] J.O. Besenhard, M.W. Wangner, M. Winter, A.D. Jannakoudakis, P.D. Jannakoudakis, E. Theodoridou, J. Power Sources 43–44 (1993) 413.
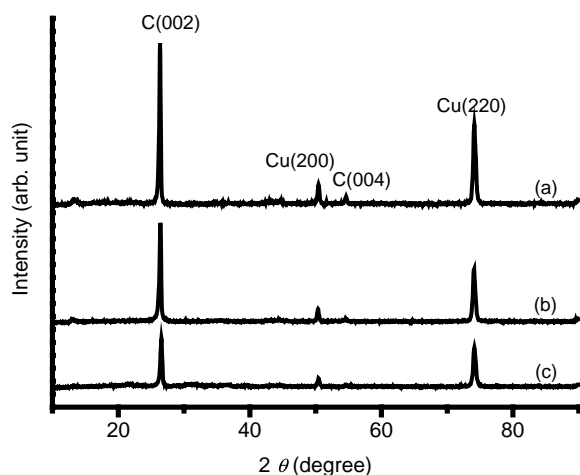[6] Y. Ein-Eli, B. Markovsky, D. Aurbach, Y. Carmeli, H. Yamin, S. Luski, Electrochim. Acta 39 (1994) 2559.

[7] J.O. Besenhard, P. Castella, M.W. Wanger, Mater. Sci. Forum 91–93 (1992) 647.

[8] B. Simon, J.P. Boeuve, M. Broussely, J. Power Sources 43–44 (1993) 65.

[9] J.O. Besenhard, M. Winter, J. Yang, W. Biberacher, J. Power Sources 54 (1995) 228.

[10] Y. Ein-Eli, S.R. Thomas, V.R. Kock, J. Electrochem. Soc. 144 (1997) 1159.

[11] M.W. Wanger, C. Liebenow, J.O. Besenhard, J. Power Sources 68 (1997) 328.

[12] M. Fujimoto, Y. Shouji, T. Nohma, K. Nishio, Denki Kagaku 65 (1997) 949.

[13] G.H. Wrodnigg, J.O. Besenhard, M. Winter, J. Electrochem. Soc. 146 (1999) 470.

[14] G.H. Wrodnigg, T.M. Wrodnigg, J.O. Besenhard, M. Winter, Electrochem. Commun. 1 (1999) 148.

[15] C. Wang, H. Nakamura, M. Yoshio, H. Yoshitake, J. Power Sources 74 (1998) 142.

[16] A. Naji, J. Ghanbaja, P. Willman, D. Billaud, Electrochim. Acta 45 (2000) 1893.

[17] Z.X. Shu, R.S. McMillan, J.J. Murrary, I.J. Davidson, J. Electrochem. Soc. 142 (1995) L161.

[18] X. Zhang, R. Kostecki, T.J. Richardson, J.K. Pugh, P.N. Ross, J. Electrochem. Soc. 148 (2001) A1341.

[19] L.G. Wade, Organic Chemistry, second ed., Prentice-Hall, Englewood Cliffs, NJ, 1991.

[20] M. Winter, J.O. Besenhard, W. Biberacher, in: J. O. Besenhard (Ed.), Handbook of Battery Materials, part III, Wily-VCH, Weinheim, 1999 (Chapter 5).

[21] R. Imhof, P. Novak, J. Electrochem. Soc. 145 (1996) 1081.

[22] PCPDFWIN, version 1.30; JCPDS X-ray Powder Data File No. 04-0836 and 41-1487, 1997.